Sustainable Energy, Grids and Networks 5 (2016) 156–166

Contents lists available at ScienceDirect

Sustainable Energy, Grids and Networks

journal homepage: www.elsevier.com/locate/segan

Islanding in distribution systems considering wind power and storage

Pilar Meneses de Quevedo [a], Javad Allahdadian [b], Javier Contreras [a,*], Gianfranco Chicco [b]

[a] E.T.S. de Ingenieros Industriales, University of Castilla - La Mancha, 13071 Ciudad Real, Spain

[b] Energy Department (DENERG), Politecnico di Torino, 10129 Torino, Italy

ARTICLE INFO

Article history:
Received 13 April 2015
Received in revised form
4 December 2015
Accepted 5 December 2015
Available online 30 December 2015

Keywords:
Islanding
Distributed generation
Distribution system
Storage devices
Two-stage stochastic programming

ABSTRACT

In modern power systems the penetration of renewable energies has been growing dramatically. The combination of renewable energy and energy storage is seen as an opportunity to better exploit the intermittent and uncertain local generation in distribution systems, especially in the case of islanding. The main goal of this paper is to keep the load and generation units on-line under islanding conditions with respect to the total power imbalance of the isolated area and minimizing the power losses and nodal voltage deviations. A two-stage stochastic linear programming model is introduced to solve the optimization problem and find the best combination of generation, demand and electrical energy storage under islanding conditions. The proposed model has been tested on a 69-bus distribution system and the results obtained in the islanded areas are presented considering two case studies (with and without electrical energy storage), under different levels of generation and demand.

1. Introduction

Currently, regulatory agencies are highly committed to increasing the integration of Renewable Energy Sources (RES) due to their global interest and benefits, including economic and ecological advantages. Likewise, several types of Energy Storage Systems (ESS) are being developed and applied in electrical networks to cope with problems such as smoothing the output power of RES [1], improving power system stability [2,3] and being economically efficient [4]. On the other hand, the penetration of RES, especially wind power, creates several problems regarding their intermittency and uncertainty [5,6]. In particular, to manage and increase the penetration of RES and ESS in electrical networks, an innovative procedure is required for both normal and abnormal conditions. Although having RES and ESS in electrical networks creates challenges to integrate them within Electrical Distribution Systems (EDS), exploiting RES and ESS in abnormal conditions like islanding can be seen as an opportunity to use more generation and demand within the island.

Islanding in power systems may be intentional or unintentional. Due to large frequency perturbations or contingency plans, intentional islanding is planned in advance in power systems to cope with problems in the network. On the other hand, unintentional islanding may occur due to the automatic response of the protection system to a fault happening in radial systems. In this case, it may be more challenging to define the islanded area conditions and guarantee the success of the islanding procedure.

In power systems, especially those with islanding conditions, supply and demand have to be balanced in real-time due to the fact that electrical energy cannot be stored efficiently in large amounts. An imbalance between supply and demand leads to several problems, such as frequency and voltage deviation in the power grid. Therefore, the definition of a predefined procedure able to keep the islanded area energized and avoid complete blackout becomes essential.

Several works have been carried out to deal with the disconnection from the bulk power system creating islands. For example, in [7–9] the configuration and control of islanding in a random way based on the topology of the grid is presented. A two-step algorithm is introduced in [10] using spectral clustering to find suitable islanding. In [11], a time domain simulation is presented to control islanding by dividing a bulk power system into several pre-selected islands. In some works, load shedding is minimized under intentional islanding conditions [12–14]. A review regarding research on planned islanding operation for a rotating type of distributed generation with a particular focus on small hydro generation is presented in [15]. A load shedding and generator tripping logic for proper islanding is developed in [16], based on detailed power system studies. An evolutionary algorithm based on current limiting protectors for controlled islands in distribution systems is presented in [17]. An islanding control approach based

* Corresponding author.
E-mail address: Javier.Contreras@uclm.es (J. Contreras).

http://dx.doi.org/10.1016/j.segan.2015.12.002
2352-4677/

Nomenclature

Indexes

i, j, k	Bus indexes
r	Piecewise linearization (PWL) block index
t	Real-time period index on a 10-min basis
ω	Scenario index

Parameters

$\hat{C}^{rs}$	Real-time storage cost of the storage unit ($/MWh)
$\hat{C}^{rp}$	Real-time production cost of the storage unit ($/MWh)
C^{sw}	Cost of switching
$d_{it\omega}$	Real power demand (MW)
f^{loss}	Power losses penalization weight factor
f^{V_dev}	Voltage deviation penalization weight factor
C^{W_curt}	Wind curtailment cost
C^{d_curt}	Real power demand curtailment cost
ini_{ij}	Initial state of switches
$\bar{I}_{ij}$	Maximum current flow through branch ij (A)
$m_{ijrt\omega}$	Slope of the rth block of the PWL
N_{loop}	Number of buses in a loop
N_B	Number of branches of the network
N_N	Number of nodes of the network
N_R	Number of blocks of the PWL
N_T	Number of time intervals
N_W	Number of scenarios
$P_{it\omega}^{d\_fore}$	Demand forecast (MW)
$P_{it\omega}^{w\_fore}$	Wind power forecast (MW)
PF_i^d	Power factor of the demand
PF_i^{wind}	Power factor of the wind turbines
$q_{it\omega}$	Reactive power demand (Mvar)
r_i^p, r_i^s	Scheduled power production/storage reserve (MW)
R_{ij}	Resistance of branch ij (Ω)
R^{tot}	Total number of blocks in the PWL
$V'^{\,2}_{it\omega}$	Approximation of the voltage magnitude of node i (kV)
V_{ref}	Nominal voltage of the distribution network (kV)
$\underline{V}$, $\overline{V}$	Minimum/maximum voltage of the distribution network (kV)
$\overline{W}^2$	Upper bound of variable $W_{ijt\omega}^2$ (kV^2)
x_0^s	Initial energy level of storage (MWh)
$\underline{x}_i$, $\bar{x}_i$	Minimum/maximum storage capacity at node i (MWh)
X_{ij}	Reactance of branch ij (Ω)
Z_{ij}	Impedance of branch ij (Ω)
$\Delta S_{ijrt\omega}$	Upper bound of the rth block of the power flow
γ	Reactive power control parameter
η_i^s, η_i^p	Efficiency rate of the storage units
Δ	Real-time period (10 min) (h)

Non-negative variables

$I_{ijt\omega}^2$	Square of the current flow through branch ij (A^2)
$P_{it\omega}^{wind}$	Real power of wind turbine at bus i (MW)
$P_{it\omega}^{dem}$	Real power of demand at bus i (MW)
$P_{it\omega}^{w\_curt}$	Real power wind curtailment at bus i (MW)
$P_{it\omega}^{d\_curt}$	Real power demand curtailment at bus i (MW)
$P_{ijt\omega}^{+}$	Real power flow (downstream) (MW)
$P_{ijt\omega}^{-}$	Real power flow (upstream) (MW)
$Q_{ijt\omega}^{+}$	Reactive power flow (downstream) (Mvar)
$Q_{ijt\omega}^{-}$	Reactive power flow (upstream) (Mvar)
$\hat{r}_{it\omega}^p$, $\hat{r}_{it\omega}^s$	Real-time production/storage reserve (MW)
$V_{it\omega}^2$	Square of the voltage magnitude of node i (kV^2)
$W_{ijt\omega}^2$	Variable related to the voltage drop (kV^2)
$\hat{x}_{it\omega}$	Storage level at node i (MWh)
$\Delta P_{ijrt\omega}$	Value of the rth block of real power (MW)
$\Delta Q_{ijrt\omega}$	Value of the rth block of reactive power (Mvar)

Free variables

$Q_{it\omega}^{wind}$	Reactive power of wind generation (Mvar)
$Q_{it\omega}^{dem}$	Reactive power of demand (Mvar)
$Q_{it\omega}^{d\_curt}$	Reactive power demand curtailment (Mvar)
$Q_{it\omega}^{wind^+}$	Reactive power upper bound of wind generation (Mvar)
$Q_{it\omega}^{wind^-}$	Reactive power lower bound of wind generation (Mvar)

Binary variables

$v_{ijt\omega}^{p+}$	Variable related to real power (upstream)
$v_{ijt\omega}^{p-}$	Variable related to real power (downstream)
$v_{ijt\omega}^{q+}$	Variable related to reactive power (upstream)
$v_{ijt\omega}^{q-}$	Variable related to reactive power (downstream)
$v_{it\omega}^s$, $v_{it\omega}^p$	Variables related to power storage or production
y_{ij}	State of the switches in branch ij: 1 if closed, 0 otherwise
$\mu_{ijrt\omega}$	State of the PWL block of real power: 0 if filled, 1 otherwise
$\eta_{ijrt\omega}$	State of the PWL block of reactive power: 0 if filled, 1 otherwise

Functions

ϕ	Total switching cost function
$\psi(\omega)$	Total cost of power losses and voltage deviation
$\kappa(\omega)$	Total costs of wind and demand curtailments and ESS operation

on the optimization of a linear DC power flow is presented in [18] and developed in [19] by implementing a piecewise linear approximation of an AC power flow. The main technical issues to develop control techniques for establishing a microgrid, in case of islanding, are addressed in [20]. In distribution systems, an island partition model with distributed generation and a two-stage branch and bound algorithm is designed in [21]. An innovative islanding feasibility function in subtransmission systems based on reactive power and real power is proposed in [22,23], respectively.

In the technical literature, an optimization procedure considering the combination of wind power with energy storage under islanding conditions in distribution systems has not been presented yet. It is worth mentioning that, due to the intermittency and uncertainty of wind power, the combination of RES and ESS is desirable in case of islanding to improve the reliability and reduce the real power imbalance between load and generation. Consequently, the motivation of this paper is to show the benefits of combining RES with ESS to minimize operational storage system costs, wind and generation curtailment, power losses and voltage deviation of buses. In other words, in this paper, a novel algorithm is presented to keep the load and generation units on-line under islanding conditions with respect to the total power imbalance of the isolated area and minimizing the power losses and nodal voltage deviations.

The study refers to the possibility of supplying the loads, without loss of generality, for a given duration, under islanding conditions after disconnection from the external grid. The basic idea proposed is that islands have to be reconnected to the main network within a given time period. In addition, due to technical reasons such as simplicity of analysis, reduction of the short circuit currents and coordination of the protections, the distribution system and the islands operate with a radial topology.

The approach of this paper is not conceived to encompass real-time control. The model is designed to balance both real and reactive power between load and generation and keep the isolated area energized. In this way, predefined control actions are defined in advance for an initial point. In order to have the right frequency in the desirable area, a balance of active power is introduced and, for voltage deviation, a reactive power balance of load and generation is considered. Consequently, the model is capable to manage the network in abnormal conditions like islanding and separation from the external grid. Of course, every ten minutes the designed model updates the setpoints for the control actions in order to consider the changes in the network after a given time step.

The mathematical formulation of this paper consists of a two-stage stochastic Mixed Integer Linear Programming (MILP) reconfiguration model considering wind energy and energy storage in EDS. Hence, an Alternative Current (AC) power flow is approximated through linear expressions to linearize the model.

Several works have been carried out to linearize the AC power flow in power system studies. In [24] an active network management strategy relying upon short-term policies to control the power of generators and load avoiding congestion or voltage problems is represented. Ref. [25] is divided in two parts. In the first part, the authors discuss about branch convexification and the misinterpretation of the physical model and unrealistic assumption therein. In the second part, two algorithms are proposed to overcome the limitations identified in the first part. A linear programming model incorporating reactive power and voltage magnitude is introduced in [26], where a piecewise linear approximation of the cosine term in the power flow equations is proposed. Two linearization techniques are implemented in [27] in the mixed non-linear programming framework to obtain an equivalent mixed integer linear programming model. In [28,29] a piecewise linear approximation function is applied to approximate the product square value of voltage and current. In [30] the demands of the electric distribution system are modeled with linear approximations in terms of real and imaginary parts of the voltage considering operating conditions of the electric distribution system. In this paper, the approaches of [28–30] are applied to obtain a linear AC power flow formulation to be introduced in the optimization problem.

Noteworthy, the linear model implemented in this paper has the following benefits: (1) is based on a robust mathematical model, (2) the computational behavior of a linear solver is more efficient than non-linear solvers and (3) using classical optimization techniques, convergence can be guaranteed.

The paper is organized as follows. In Section 2, a stochastic model of wind and a generic model of storage system is introduced. Section 3 describes the optimization problem formulated as a stochastic MILP. The case studies are illustrated and explained in Section 4. Results and discussion are presented in Section 5. Finally, Section 6 contains the conclusions.

2. Wind generation and storage units modeling

2.1. Wind production uncertainty modeling

With the expected growth of wind power penetration in electrical networks, it is necessary to consider the intermittency and uncertainty of these resources. Therefore, in order to model wind uncertainty, a probabilistic method based on time series has been implemented, according with the principles indicated in [31].

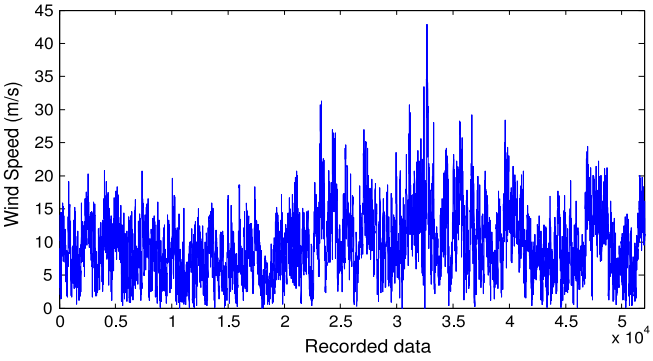

Fig. 1. Historical wind speed data for one year.

Historical data of one year of wind generation [32] are considered as initial data (Fig. 1) and represented through their Cumulative Distribution Function (CDF). Starting from the initial data, in this paper the empirical distribution functions are used instead of constructing Beta distribution functions as in [31]. In this way, the full statistical characteristics of the initial data are preserved. This is the only difference with respect to the procedure applied in [31] for creating a number of wind speed patterns.

The application of the procedure contains the following steps:

(a) Preparatory phase: from the CDF of the historical wind speed, the wind speeds are partitioned into deciles, obtaining the corresponding wind speed ranges with the following upper values: 3.875, 5.425, 6.717, 7.879, 9.171, 10.463, 11.755, 13.434, 16.017 and 42.885 m/s. Then, taking all the wind speeds located in the same decile, the CDF representing the wind speed at the next time step is constructed (all the wind speeds of the next time step reached by starting from a wind speed in the same decile are used to form the CDF).

(b) Choice of the number of scenarios and selection of the initial wind speed: N_W wind speed patterns are constructed, each one starting from a wind speed value randomly selected from the probability distribution of the historical data. The selection mechanism is the classical one, consisting of extracting for each scenario a random number from a uniform probability distribution in (0, 1), entering the CDF of the historical wind speed with that random number and identifying the corresponding wind speed.

(c) Construction of the wind speed time series for each scenario: the decile of the initial wind speed is identified. The CDF of the wind speed at the next time step for that decile is considered, extracting the wind speed from that CDF with the classical selection mechanism indicated above. The decile of the wind speed extracted is identified, the corresponding CDF of the next time step is considered, the new wind speed is extracted, and so forth until all the wind speed values in the time interval of analysis have been extracted.

By using this procedure, the evolution of the individual generated patterns is representative of the evolution of the pattern in the historical data set. In order to show the effectiveness of this procedure, Fig. 2 visualizes the reordered historical data with one-year data at 10-min time steps (thick line), together with the reordered data of 12 patterns constructed for the same one-year duration and 10-min time steps. It is apparent that the sequence of reordered data is quite close to the one of the reordered historical data.

In this paper, the islanding period considered is relatively short (e.g., one hour), and the quantity of interest is the wind

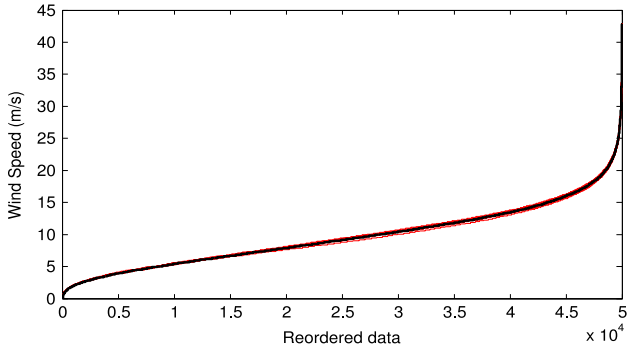

Fig. 2. Reordered wind speed for one year.

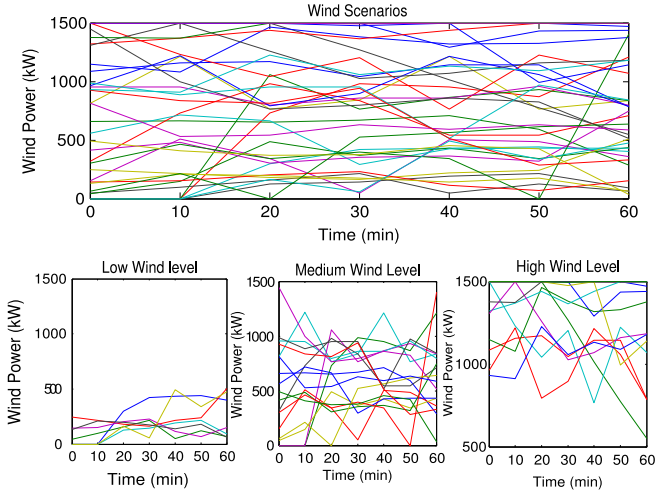

Fig. 3. Different levels of wind and demand in islanded areas.

power obtained from the wind speed by using the manufacturer's curve [33]. For the purpose of the analysis, the N_W wind speed patterns correspond to N_W wind power scenarios, and these scenarios are further grouped into three wind levels (namely, low, medium and high), defined on the basis of the CDF of the average wind speed resulting from the wind speed patterns (Fig. 3). In particular, the lowest 1/3 of wind speeds are associated with the low wind level, the highest 1/3 of wind speeds are associated with the high wind level, and the remaining ones are associated with the medium wind level.

2.2. Generic storage unit model

Several forms of ESS have been identified in EDS, meeting different goals including improving power system reliability, feeding real-time power demand and being economically efficient. In this paper, a generic storage unit model is introduced and applied [34]. The mathematical formulation of the ESS is represented through (1)–(6).

$$0 \le \hat{r}^p_{it\omega} \le r^p_i v^p_{it\omega} \tag{1}$$

$$0 \le \hat{r}^s_{it\omega} \le r^s_i v^s_{it\omega} \tag{2}$$

$$\underline{x}_i \le \hat{x}_{it\omega} \le \bar{x}_i \tag{3}$$

$$\hat{x}_{it\omega} = \hat{x}_{i(t-1)\omega} + \Delta[\eta^s_i \hat{r}^s_{it\omega} - (1/\eta^p_i)\hat{r}^p_{it\omega}] \tag{4}$$

$$\hat{x}_{it\omega=0} = x^s_0 \tag{5}$$

$$v^p_{it\omega} + v^s_{it\omega} \le 1. \tag{6}$$

In the above equations, the actual reserve bounds are defined in (1) and (2). The capacity limits of the ESS is introduced by (3). Eq. (4) shows the storage transition function. Thus, the state of charge, $\hat{x}_{it\omega}$ (storage level at node i, period t and scenario ω), of the ESS located at bus i at the end of time interval t for each scenario ω depends on the previous state of charge, $\hat{x}_{i(t-1)\omega}$, and the power storage/production during the current interval. The initial energy status of the ESS is defined in (5). Finally, in (6), binary variables $v^p_{it\omega}$ and $v^s_{it\omega}$ are defined and added to (1) and (2) to avoid producing and storing energy simultaneously.

3. Stochastic formulation of the problem

The following assumptions are defined to represent the simplified operation of EDS including switches, generation and storage devices:

- The EDS is a balanced three-phase system and can be represented by its equivalent single-phase circuit.
- Shunt line parameters are not considered.
- The islanding duration is predefined. The islanding period is partitioned into time intervals denoted with t. The duration of the time intervals depends on data availability.
- The coupling time of ESS is 10 min (6 time intervals during 1 h).
- Changes in the load patterns in the EDS may occur for each time interval. Inside each time interval all the variables are assumed to be constant.
- The location of storage units has already been defined in the planning phase.
- Losses in the ESS are ignored.

3.1. Objective function

The objective function is formulated by using two-stage stochastic programming as shown in (7)–(10). At the first stage, the costs of switching under islanding conditions regardless of the scenarios ϕ are defined in (8). There, the first term is related to the cost of closing a switch in branch i, j and the second refers to the cost of opening a switch in branch i, j. Noteworthy, at this stage, the status of the switches are defined and will not change during islanding periods. At the second stage, regarding the scenarios, the expected values of the total cost of the real power losses and the voltage deviation with respect to the reference value, $\psi(\omega)$, in branch i, j are penalized in (9). Likewise, the cost of generation and demand curtailment and the real-time production/storage cost in the ESS located at bus i, $\kappa(\omega)$ are considered in (10), for each time interval t, with respect to the different scenarios (ω) and islanding conditions.

At the first stage, the variables are only related to the behavior of the switches, which remains invariant during the whole hour, and at the second stage, other variables are related to scenarios.

$$\min\{\phi + E[\psi(\omega)] + E[\kappa(\omega)]\} \tag{7}$$

$$\phi = \sum_{ij}(y_{ij}C^{sw})\Big|_{ini_{ij}=0} + \sum_{ij}((1-y_{ij})C^{sw})\Big|_{ini_{ij}=1}. \tag{8}$$

In (8), the first and second terms refer to open and closed switches before islanding, respectively.

$$\psi(\omega) = \Delta\left[\sum_t\sum_{ij} R_{ij}I^2_{ijt\omega}f^{loss} + \sum_t\sum_{ij}\left|V^2_{it\omega} - V^2_{ref}\right|f^{V_{dev}}/R_{ij}\right] \tag{9}$$

$$\kappa(\omega) = \Delta\left[\sum_t\sum_i (P^{w\_curt}_{it\omega}C^{w\_curt}_{it\omega} + P^{d\_curt}_{it\omega}C^{d\_curt}_{it\omega} + \hat{r}^p_{it\omega}\hat{C}^{rp} + \hat{r}^s_{it\omega}\hat{C}^{rs})\right]. \tag{10}$$

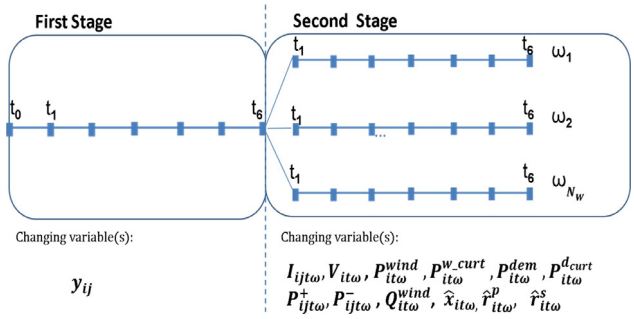

Fig. 4. Two-stage objective function.

The voltage deviation is formally expressed as (11). However, in order to use $V_{it\omega}^2$ as a variable in the MILP model, an approximation is introduced by considering $V_{it\omega} = V_{ref}$ in the last term of (11), as seen in (12).

$$(V_{it\omega} - V_{ref})^2 = \left|V_{it\omega}^2 + V_{ref}^2 - 2V_{it\omega}V_{ref}\right| \tag{11}$$

$$\left|V_{it\omega}^2 + V_{ref}^2 - 2V_{it\omega}V_{ref}\right| = \left|V_{it\omega}^2 - V_{ref}^2\right|. \tag{12}$$

Fig. 4 illustrates the two-stage objective function. In the first stage, the status of the switches is defined regardless of scenarios and time; in the second stage, several variables are characterized as indicated in the figure.

3.2. Constraints

Various constraints are included in the following mathematical statements to assure optimal operation conditions.

3.2.1. Real-time power balance equations

Eq. (13) is formulated to be implemented in the power balance equation (15).

$$P_{it\omega}^{dem} = P_{it\omega}^{d\_fore} - P_{it\omega}^{d\_curt}. \tag{13}$$

As assumed, wind turbines are able to compensate the reactive power in order to maintain the grid security under islanding conditions. The wind power balance is formulated in (14) and implemented in (15).

$$P_{it\omega}^{wind} = P_{it\omega}^{w\_fore} - P_{it\omega}^{w\_curt}. \tag{14}$$

Real and reactive power balances at node i are formulated in (15) and (16), respectively.

In order to determine the direction of the current and power flow (forward or backward), especially in (15) and (16), two types of positive separate variables applied to both active power ($P_{ijt\omega}^{+}$, $P_{ijt\omega}^{-}$) and reactive power ($Q_{ijt\omega}^{+}$, $Q_{ijt\omega}^{-}$) are introduced in Fig. 5. Wind power generation, storage/production of ESS and, demand power curtailment and power losses are considered in these constraints.

$$P_{it\omega}^{wind} + \sum_{k}(P_{kit\omega}^{+} - P_{kit\omega}^{-}) - \sum_{j}[(P_{ijt\omega}^{+} - P_{ijt\omega}^{-}) + R_{ij}I_{ijt\omega}^2] + (\hat{r}_{it\omega}^{p} - \hat{r}_{it\omega}^{s}) = P_{it\omega}^{dem} \tag{15}$$

$$Q_{it\omega}^{wind} + \sum_{k}(Q_{kit\omega}^{+} - Q_{kit\omega}^{-}) - \sum_{j}[(Q_{ijt\omega}^{+} - Q_{ijt\omega}^{-}) + X_{ij}I_{ijt\omega}^2] = Q_{it\omega}^{dem}. \tag{16}$$

3.2.2. Voltage drop equations

Voltage drops between nodes are formulated in (17), where $W_{ijt\omega}^2$ is an auxiliary variable related to switching operations. In case of open switching at branch i, j, $W_{ijt\omega}^2$ takes into account that there is a voltage drop between bus i and bus j.

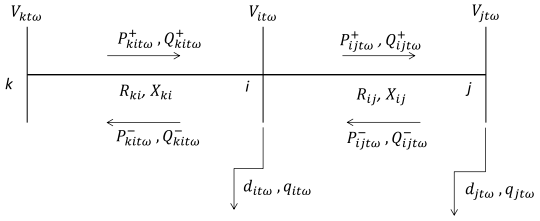

Fig. 5. Illustrative radial distribution system.

$$V_{it\omega}^2 - Z_{ij}^2 I_{ijt\omega}^2 - V_{jt\omega}^2 + W_{ijt\omega}^2 - 2[R_{ij}(P_{ijt\omega}^{+} - P_{ijt\omega}^{-}) + X_{ij}(Q_{ijt\omega}^{+} - Q_{ijt\omega}^{-})] = 0. \tag{17}$$

The maximum and minimum voltage variations for bus i are defined in (18). Constraints (19) and (20), state that auxiliary variable $W_{ijt\omega}$ is 0 when branch i, j is in operation ($y_{ij} = 1$). Moreover, $\overline{W}^2$ must be calculated to give enough freedom for variable $W_{ijt\omega}^2$ in order to satisfy constraint (17). The upper bound of this variable is the difference of the square values of the maximum and minimum voltages of the network.

$$\underline{V}^2 \le V_{it\omega}^2 \le \overline{V}^2 \tag{18}$$

$$W_{ijt\omega}^2 \ge -\overline{W}^2(1 - y_{ij}) \tag{19}$$

$$W_{ijt\omega}^2 \le \overline{W}^2(1 - y_{ij}). \tag{20}$$

3.2.3. Current and power magnitude limits

A set of constraints is represented regarding the thermal limits of the EDS. Constraints (21), (22)–(23) and (24)–(25) are introduced for the current, real and reactive power bounds, respectively. Finally, (26) and (27) are set to avoid considering forward and backward power flows simultaneously. Note that (22)–(25) are auxiliary constraints to improve the convergence of the proposed model.

$$0 \le I_{ijt\omega}^2 \le \bar{I}_{ij}^2 y_{ij} \tag{21}$$

$$P_{jit\omega}^{+} \le V_{nom}\bar{I}_{ij}v_{ijt\omega}^{P+} \tag{22}$$

$$P_{jit\omega}^{-} \le V_{nom}\bar{I}_{ij}v_{ijt\omega}^{P-} \tag{23}$$

$$Q_{jit\omega}^{+} \le V_{nom}\bar{I}_{ij}v_{ijt\omega}^{Q+} \tag{24}$$

$$Q_{jit\omega}^{-} \le V_{nom}\bar{I}_{ij}v_{ijt\omega}^{Q-} \tag{25}$$

$$v_{ijt\omega}^{P+} + v_{ijt\omega}^{P-} \le y_{ij} \tag{26}$$

$$v_{ijt\omega}^{Q+} + v_{ijt\omega}^{Q-} \le y_{ij}. \tag{27}$$

3.2.4. Non-linear apparent power equations

The current flow magnitude is formulated in (28), which is the only non-linear equation in the optimization problem. The linearization procedure is explained in detail in Section 3.3.

$$V_{it\omega}^2 I_{ijt\omega}^2 = P_{ijt\omega}^2 + Q_{ijt\omega}^2. \tag{28}$$

3.2.5. Radiality constraints

Constraint (29) is designed to configure the network in a radial form, which means the number of closed branches in any loop has

to be less than the total number of branches in that loop, as in [35]. The detailed description of the algorithm is presented in [36]. Initially, a Depth-First Search strategy is used to detect all the loops in the network, assuming that the switches are closed. This strategy discovers paths in the network as a sequence of nodes. Therefore, a loop is defined as a closed path with no repeated node excluding the first and last points. In order to maintain the radiality of the system, there should be at least one open branch in each potential loop.

$$\sum_{ij} y_{ij} \leq N_{loop} - 1. \tag{29}$$

3.2.6. Wind reactive power equations

In order to coordinate real and reactive power, the limitations of reactive power for wind turbines are calculated in (29), where $\gamma \geq 1$ is a user-defined coefficient.

$$Q_{it\omega}^{wind^-} = P_{it\omega}^{wind}(\tan(\arccos(-PF_i^{wind}))) \tag{30}$$

$$Q_{it\omega}^{wind^+} = P_{it\omega}^{wind}(\tan(\arccos(PF_i^{wind}))) \tag{31}$$

$$Q_{it\omega}^{wind^-} \leq Q_{it\omega}^{wind} \leq Q_{it\omega}^{wind^+} \tag{32}$$

$$Q_{it\omega}^{wind^+} - Q_{it\omega}^{wind^-} \geq \gamma Q_{it\omega}^{dem}. \tag{33}$$

To apply constraint (33), as mentioned in [22], the islanded area should be divided into reactive control parts, based on the electrical distance measured in the network. However, as the reactive power demand can be compensated by generators and the voltage deviation of the nodes with respect to the reference value is already considered in the model, the separation of the network into islanded areas, based on the mentioned method, is skipped here. In this way, the network is divided into 3 predefined islanded areas regarding the location of the generators and their ability to compensate reactive power for local loads.

3.3. PWL procedure

The mathematical model implemented in this paper is nonlinear due to the constraint appearing in (28). In order to create a linear model, the PWL methods proposed in [28–30] are used here. To create a linear equation from constraint (28), the two sides of the equation should be handled separately. Note that $V_{it\omega}^2$ and $I_{ijt\omega}^2$ are variables that represent the square magnitude values of voltages and currents respectively and they are implemented in (15)–(18) and (21). The linearization process of Eq. (28) is described as follows.

- $V_{jt\omega}^2 I_{ijt\omega}^2$: The left side of (28) is handled by splitting $V_{jt\omega}^2$ into small segments. However, this leads to an increase in the number of binary variables and computation time. In EDS voltage magnitudes are within a small range, so a constant value V_{ref}^2 can be considered as voltage magnitude for the first run of the model in which binary variables are relaxed [28], as shown in (34).

  $$V_{jt\omega}^2 I_{ijt\omega}^2 \approx V_{ref}^2 I_{ijt\omega}^2. \tag{34}$$

  Then, the model is run again and $V_{jt\omega}^2$ takes the value resulting from the first run. Note that $V_{jt\omega}^2$ hardly changes after the second execution. Due to the limited range of voltage magnitude variation, this simplification is approximated with a small error.
- $P_{ijt\omega}^2 + Q_{ijt\omega}^2$: Both terms on the right side of (28) are handled by introducing a piecewise linear approximation [29,30]. The process of linearization is presented as follows:

$$P_{ijt\omega}^2 + Q_{ijt\omega}^2 = \sum_r (m_{ijrt\omega} \Delta P_{ijrt\omega}) + \sum_r (m_{ijrt\omega} \Delta Q_{ijt\omega}) \tag{35}$$

$$P_{ijt\omega}^+ + P_{ijt\omega}^- = \sum_r \Delta P_{ijrt\omega} \tag{36}$$

$$Q_{ijt\omega}^+ + Q_{ijt\omega}^- = \sum_r \Delta Q_{ijrt\omega} \tag{37}$$

$$0 \leq \Delta P_{ijrt\omega} \leq \Delta S_{ijrt\omega} \tag{38}$$

$$0 \leq \Delta Q_{ijrt\omega} \leq \Delta S_{ijrt\omega} \tag{39}$$

where:

$$m_{ijrt\omega} = (2r - 1)\Delta S_{ijrt\omega} \tag{40}$$

$$\Delta S_{ijrt\omega} = (V_{nom} \bar{I}_{ij})/R_{ij}. \tag{41}$$

Eq. (35) is a piecewise linear approximation of $(P_{ijt\omega}^2 + Q_{ijt\omega}^2)$, and (36) and (37) represent that $(P_{ijt\omega}^+ + P_{ijt\omega}^-)$ and $(Q_{ijt\omega}^+ + Q_{ijt\omega}^-)$ are equal to the sum of the values in each block of the discretization, which means they are a set of linear terms. In addition, $m_{ijrt\omega}$ and $\Delta S_{ijrt\omega}$ are constant parameters and, (36) and (37) are a set of linear expressions. Therefore, (42) represents the final linear form of constraint (28). In this equation, $V_{jt\omega}^2$ is a parameter and $\sum_r (m_{ijrt\omega} \Delta P_{ijrt\omega})$ and $\sum_r (m_{ijrt\omega} \Delta Q_{ijrt\omega})$ are linear. Fig. 6 shows the PWL of $P_{ijt\omega}^2$.

The model is linear since a PWL has been performed, so, the solution is a global optimum. By increasing the number of blocks, the solution is more accurate, however, the computation time also increases. As performed in several experimental simulations, the solutions hardly change from 20 blocks onwards in the piecewise linear procedure.

$$V_{ref}^2 I_{ijt\omega}^2 = \sum_r (m_{ijrt\omega} \Delta P_{ijrt\omega}) + \sum_r (m_{ijrt\omega} \Delta Q_{ijrt\omega}). \tag{42}$$

In Refs. [28–30] the authors show a set of performance assessments of the approximate method compared with an accurate linearized power flow model (AC). The authors conclude that the error obtained using the piecewise linear approximation may reach a maximum percentage error of 1%.

There are two ways to carry out the PWL of $P_{ijt\omega}^2$ (and also $Q_{ijt\omega}^2$), the one that uses binary variables and another one that does not use them. The use of binary variables to identify in which straight-line of the linearization $P_{ijt\omega}$ is located (when calculating $P_{ijt\omega}^2$) is the most efficient, robust and accurate method, but it is necessary to include many additional binary variables in the model that produce an increase in the computational effort. If no binary variables are used in the linearization, relaxing the adjacency condition is needed to ensure the correct performance of the PWL (see Appendix).

4. Case studies

To assess the behavior of the network in several situations, the proposed model is applied on a 69-bus network. The data of the network is collected from [37]. The maximum current flow in all the lines and the upper bound $\overline{W}^2$ of the auxiliary variable related to the voltage drop are, 90 A and 0.4 kV^2, respectively. Due to the location of loads and generators, the probability of islanding in three areas of the network is anticipated. Therefore, the network is divided into three predefined islanded areas. In particular, the three predefined islanded areas and the location of wind turbines and storage units are represented in Fig. 7. Network specifications are shown in Table 1. In the PWL, 20 discrete blocks are considered.

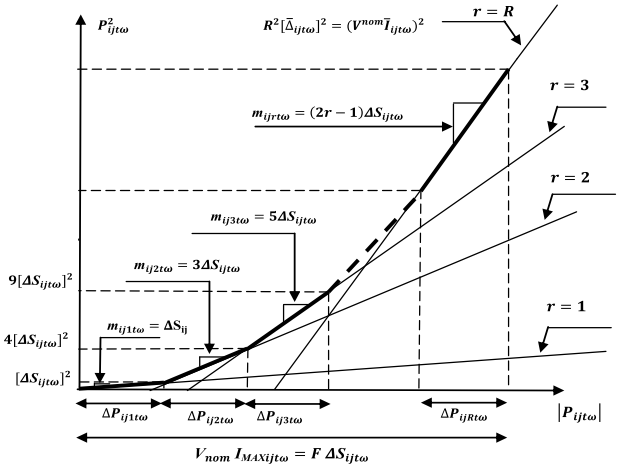

Fig. 6. Modeling the piecewise linear function $P^2_{ijt\omega}$.

The upper and lower voltage limits of the buses are 1.1 and 0.9 pu, respectively. The islanding duration considered is 1 h.

Demand data, recorded every 10 min, is collected from the Iberian Electricity Market [38]. Wind generation data are taken from historical records having 10 min time step. On these bases, the islanding duration is divided into 10-min time intervals (6 time intervals). In the PWL procedure described in Section 3.3, 20 discrete blocks are considered.

Three levels of wind generation are combined with 3 levels of demand to create 9 cases. Accordingly, for demand, 20%, 100% and 180% of the average values from historical data are defined as different levels. For wind power, $N_W = 50$ scenarios are constructed and three wind power levels (low, medium and high) are defined as indicated in the last part of Section 2.1. Furthermore, for a better analysis, two different case studies are considered: (A) only wind generation and (B) wind generation along with storage units. The combination of different levels of power for wind generation and demand produces 9 cases. Consequently, every case is applied for both case studies in order to find out the behavior of the network and analyze various results. The capacity of each storage unit is 0.15 MW and the initial energy level is set to 50% of their capacities (0.075 MW). Also, the upper and lower bounds of storage/production in each storage system are 0.15 MW and 0 MW, respectively.

Table 1
Network characteristics considering three islands (kW).

Island	1st	2nd	3rd	Total
Average demand (20%)	6.04	71.03	143.79	220.86
Average demand (100%)	30.19	355.19	718.95	1104.33
Average demand (180%)	54.35	639.34	1294.12	1987.81
Average low wind level	39.98	79.97	79.97	199.92
Average med wind level	122.75	245.51	245.51	613.77
Average high wind level	263.54	527.07	527.07	1317.68
Storage capacity	75	150	75	300
Number of switches	0	4	1	5

5. Results and discussion

For the 9 cases defined, Tables 2–4 represent the results of the optimization problem considering different cases under islanding conditions for islands 1, 2 and 3, respectively. The initial load and generation for each case before being disconnected from the external grid are shown in the first section of the tables. The results, including connected loads and generators, stored/produced energy and power losses, are illustrated in the remaining two sections of each table, showing the islanded area results in presence of ESS and the results without ESS, respectively.

Since the only energy source under islanding conditions is wind, there are three possibilities: (1) wind generation higher than demand, (2) demand higher than wind and, (3) balanced wind and demand. As the network is analyzed with and without ESS, several situations and conditions are expected.

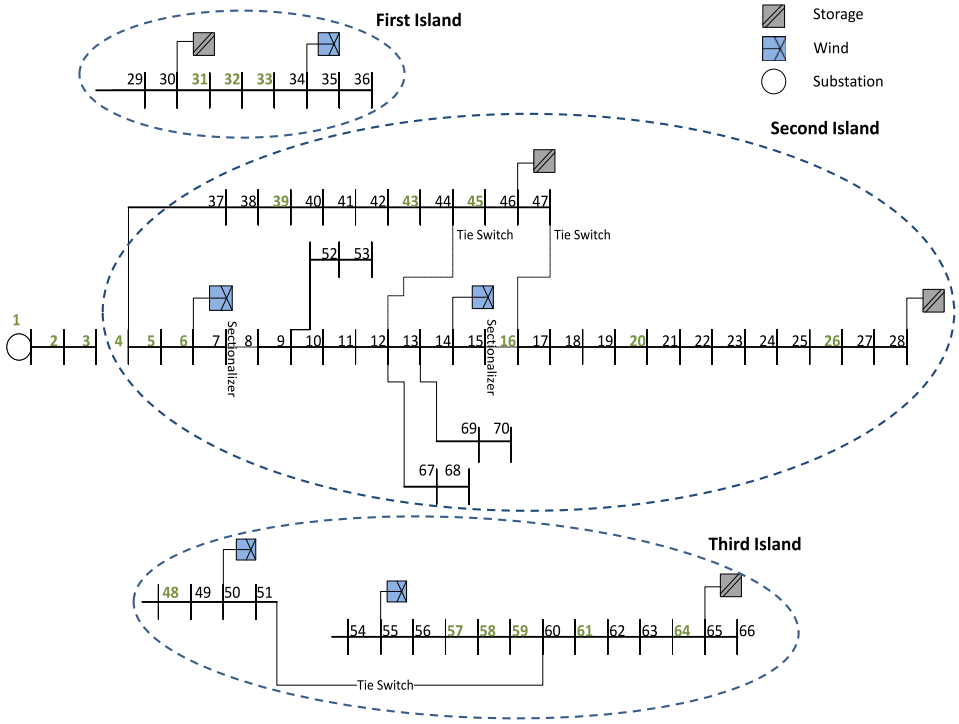

Fig. 7. Network and island configurations.

Table 2
Island 1 results (values in kW).

Island 1 (cases)		1	2	3	4	5	6	7	8	9
Total initial load		6.04	30.19	54.35	6.04	30.19	54.35	6.04	30.19	54.35
Total initial generation		39.98	39.98	39.98	122.75	122.75	122.75	263.54	263.54	263.54
Islanding without ESS										
Load		5.60	24.82	33.47	5.80	28.56	50.93	6.04	30.19	54.35
Generation (wind)		5.95	25.94	34.21	6.16	30.31	54.02	6.41	32.06	57.72
Power losses		0.35	1.12	0.74	0.36	1.74	3.09	0.37	1.87	3.37
Islanding with ESS										
Load		6.04	30.19	54.35	6.04	30.19	54.35	6.04	30.19	54.35
Generation (wind)		38.84	39.98	39.98	75.78	91.89	104.73	79.30	133.39	127.20
Storage	Produces	0.13	3.81	18.08	0.24	1.63	3.42	0.36	1.78	3.20
	Stores	32.74	13.09	3.46	67.56	60.64	51.00	70.59	70.59	70.40
Power losses		0.19	0.51	0.26	2.42	2.69	2.80	3.03	4.38	5.65

Table 3
Island 2 results (values in kW).

Island 2 (cases)		1	2	3	4	5	6	7	8	9
Total initial load		71.04	355.19	639.35	71.04	355.19	639.35	71.04	355.19	639.35
Total initial generation		79.97	79.97	79.97	245.51	245.51	245.51	527.07	527.07	527.07
Islanding without ESS										
Load		55.12	79.90	79.92	66.17	235.23	245.17	71.04	329.29	524.24
Generation (wind)		58.61	79.97	79.97	72.36	239.18	245.51	72.07	331.52	527.07
Power losses		3.49	0.07	0.04	6.18	3.94	0.34	1.03	2.23	2.83
Islanding with ESS										
Load		71.04	229.71	229.93	71.04	333.86	395.22	71.04	355.19	616.47
Generation (wind)		79.97	79.97	79.97	94.56	245.51	245.51	220.46	429.02	527.07
Storage	Produces	15.61	150	150	29.74	100.14	150	0	58.32	92.66
	Stores	24.33	0	0	49.23	9.57	0	148.44	130.92	0.87
Power losses		0.21	0.25	0.04	4.03	2.21	0.29	0.98	1.23	2.39

Table 4
Island 3 results (values in kW).

Island 3 (cases)		1	2	3	4	5	6	7	8	9
Total initial load		143.79	718.96	1294.12	143.79	718.96	1294.12	143.79	718.96	1294.12
Total initial generation		79.97	79.97	79.97	245.51	245.51	245.51	527.07	527.07	527.07
Islanding without ESS										
Load		71.93	79.61	79.77	127.70	241.43	242.46	143.11	511.65	512.18
Generation (wind)		73.37	79.97	79.97	135.92	245.51	245.51	151.15	527.07	527.07
Power losses		1.44	0.36	0.20	8.22	4.08	3.05	8.04	15.43	14.89
Islanding with ESS										
Load		143.79	154.76	154.86	134.16	318.23	318.73	143.74	587.81	594.41
Generation (wind)		79.97	79.97	79.97	184.9	245.51	245.51	230.89	523.36	527.07
Storage	Produces	71.34	75	75	5.03	75	75	0	75	75
	Stores	3.66	0	0	49.68	0	0	75	0	0
Power losses		3.85	0.20	0.11	6.09	2.27	1.78	12.15	10.54	7.66

5.1. Islanding without ESS

In the case of islanding without ESS, if the amount of load is higher than generation, the optimization procedure disconnects part of the load in order to keep the real power imbalance within acceptable limits (Fig. 8(a)). Also, with a surplus of generation, the optimization model tries to balance the power in the islanded area by decreasing power generation in that area (Fig. 8(b)). In a few cases, the power imbalance between load and generation is very low and depends on the stochastic inputs of the load and generation, the optimization model tries to shed both of them. This happens mostly in cases 2, island 1 and in cases 1, 5, 8 and 9, island 2, as it can be seen in Table 3 and in case 1, shown in Fig. 8(c).

5.2. Islanding with ESS

In the presence of both wind and storage, several situations are likely to happen in the case of islanding. With an excess of wind generation in the islanded area, three different situations can occur. The first situation occurs when wind generation is higher than the load plus the total storage capacity (Fig. 8(d)). In this case, wind curtailment is unavoidable in every interval and the ESS is fully charged. The second situation occurs when the surplus of generation can be completely stored by the ESS in one hour, thus, avoiding any curtailment. This is the same situation seen in Fig. 8(b), but considering ESS to store the excess of wind generation. However, in the third situation, it may be necessary to disconnect generation in some time intervals due to

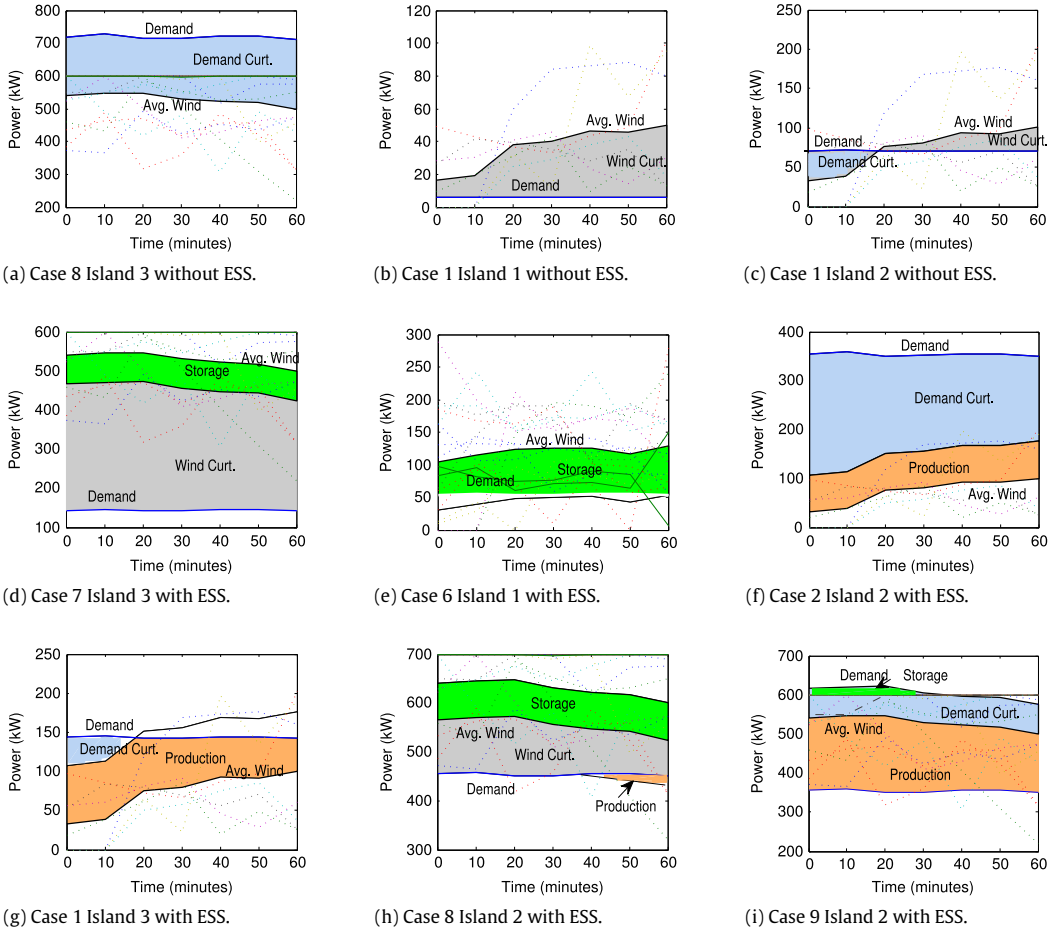

(a) Case 8 Island 3 without ESS. (b) Case 1 Island 1 without ESS. (c) Case 1 Island 2 without ESS.

(d) Case 7 Island 3 with ESS. (e) Case 6 Island 1 with ESS. (f) Case 2 Island 2 with ESS.

(g) Case 1 Island 3 with ESS. (h) Case 8 Island 2 with ESS. (i) Case 9 Island 2 with ESS.

Fig. 8. Islanding power balance situations; (Blue: demand curtailment; Gray: wind curtailment; Green: energy storage for ESS; Orange: energy production for ESS). The dashed lines represent the wind scenarios for the corresponding wind level. (For interpretation of the references to color in this figure legend, the reader is referred to the web version of this article.)

extra generation in that time interval (Fig. 8(e)) i.e., for that 10 min interval, the storage capacity of the ESS is lower than generation and, within this time interval, it is not possible to store energy.

On the other hand, several situations can be analyzed in the case of an excess of demand. In several cases, generally in islands 2 and 3, the total stored energy in ESS is used to compensate the imbalance of power in islanding conditions. However, some loads should be disconnected in order to balance the power (Fig. 8(f) and (g)). In other cases, the ESS injects part of its capacity into the network, which is enough to compensate the power in that area, avoiding any demand curtailment (case 8 in island 3 with ESS) and it is similar to Fig. 8(a), in which the deficit of wind power generation is compensated by the storage production.

Finally, other situations can occur depending on the amount of imbalance between load and generation and the capacity of the ESS. For instance, in cases 8 and 9 of island 2, the ESS produces or stores energy depending on the time interval (Fig. 8(h) and (i)).

5.3. General islanding analysis

Table 2 shows the results of the optimization problem after the disconnection of island 1. The minimum and maximum initial power imbalances in this area are 9.79 kW and 257.5 kW, respectively.

The output of the optimization model for island 2 is illustrated in Table 3. The minimum and maximum initial power imbalances are 8.93 kW and 559.38 kW and they are related to cases 1 and 3, respectively. Unlike other islands, two ESS with a total capacity of 150 kW are connected to this area. In cases 2, 3 and 6 the energy is fully produced by the ESS. On the other hand, only in case 7, the energy is completely stored by the ESS. Noteworthy, in cases 1, 5, 8 and 9, the energy is stored or produced by the ESS depending on the level of wind power or demand in the time intervals. The minimum and maximum power losses are 0.04 kW and 6.18 kW, respectively, and they are related to cases 3 and 4, respectively.

Finally, Table 4 presents the results of the optimization model for island 3. The minimum and maximum initial power imbalances are 63.14 kW in case 1 and 1214.15 kW in case 3, respectively. This islanded area has the highest level of power imbalance in case 3 compared with the other islanded areas. Consequently, the ESS will be fully charged or discharged regarding the amount of power imbalance in the islanded area. Although, in some cases, the energy can be stored or produced by the ESS completely, a small part of generation or demand is disconnected and the ESS cannot avoid disconnecting them. As the reactive power is not compensated by the ESS, in some cases, e.g. cases (1 and 4) a curtailment of generation or demand is unavoidable. Finally, the minimum and maximum power losses are 0.11 kW in case 3 and 15.43 kW in case 8, respectively.

In general, generation and demand curtailment are lower in the presence of ESS in islanded areas. Since power losses are related to the location of load and generation and the limitation of the connection lines in EDS, lower power losses with ESS are not guaranteed.

Regarding the reactive power imbalance in the network, in all cases and islanded areas, the generation is able to compensate the reactive power after islanding and the optimization procedure.

Table 5
Order of complexity.

	Without ESS	With ESS
Binary variables	$4N_B\,N_T\,N_W + N_B$	$4N_B\,N_T\,N_W + 2N_N\,N_T\,N_W + N_B$
Continuous variables	$8N_B\,N_T\,N_W + 10N_N\,N_T\,N_W$	$8N_B\,N_T\,N_W + 12N_N\,N_T\,N_W$
Constraints	$19N_B\,N_T\,N_W + 11N_N\,N_T\,N_W$	$19N_B\,N_T\,N_W + 17N_N\,N_T\,N_W$

Table 6
Order of complexity using binary variables in the PWL.

	Without ESS	With ESS
Binary variables	$4N_B\,N_T\,N_W + N_B + 2N_B\,N_R\,N_T\,N_W$	$4N_B\,N_T\,N_W + 2N_N\,N_T\,N_W + N_B + 2N_B\,N_R\,N_T\,N_W$

Reactive power is introduced as a constraint in the optimization model and power losses are lower than the optimization model including reactive power in the objective function.

5.4. Scalability of the model

All the cases have been solved using MATLAB R2012a [39] and CPLEX under GAMS 24.0 [40] on a Windows 8-based Dell Server R920 with four processors Intel Xeon E7-4820 clocking at 2 GHz and 128 GB of RAM. Table 6 illustrates the comparison between the order of complexity of the model with and without ESS. The number of binary and continuous variables and constraints depends on the number of nodes (N_N), the number of branches (N_B), the number of time intervals (N_T) and the number of scenarios (N_W). In Table 5, the characterization of the model is illustrated.

6. Conclusion

In this paper, a two-stage stochastic MILP reconfiguration model considering wind energy and ESS in EDS has been implemented in order to maximize load and generation under islanded conditions. The objective function of the optimization model has been based on real power with additional constraints for reactive power in the islanded area. The output of the mathematical model has been analyzed by using 9 cases in 3 islanded areas including wind generation and ESS. The proposed model leads to correct operation of the grid in islanded situations and avoids a complete blackout in these areas under different levels of generation and demand. The EDS network has been analyzed by considering wind generation only and with a combination of wind and ESS are analyzed. It has been observed that the combination of wind generation and ESS leads to keeping more load and generation on-line under islanded conditions.

Acknowledgment

This work has been funded by the EU Seventh Framework Programme FP7/2007–2013, under grant agreement no. 309048 (Project SiNGULAR).

Appendix. PWL process

The implementation of the PWL within an optimization framework generally requires binary integer variables to enforce adjacency conditions for the piecewise linear segments. Adjacency conditions ensure that $P_{ijrt\omega} \geq 0$ if $P_{ij(r-1)t\omega} = \Delta S_{ijrt\omega}$.

However, omitting binary variables and relaxing the adjacency condition provide a strictly continuous linear approximation of $P^2_{ijt\omega}$ and $Q^2_{ijt\omega}$ that is equivalent to a bounded convex relaxation of (28) as in (43). The adjacency of the power blocks does not need to be enforced explicitly as in [41,42]. It has been verified that (43) is active in the solution.

$$V^2_{it\omega} I^2_{ijt\omega} \geq P^2_{ijt\omega} + Q^2_{ijt\omega}. \tag{43}$$

The proof, as mentioned in [43], is that the function $P^2_{ijt\omega}$ is strictly convex (is the same for $Q^2_{ijt\omega}$) if the Hessian is positive definite ($\nabla^2(P^2_{ijt\omega}) \geq 0$), which is the case.

All of this has been checked experimentally by including binary variables, and the solution has not changed. Yet, by introducing binary variables the computational time increases. This increase has been expressed by determining the computational complexity of the models, as follows, by using the variables already introduced in this paper and adding the number of blocks, N_R, as seen in Table 6.

For the sake of completeness, in order to show the use of binary variables, the new equations that include binary variables are presented as done in [44].

$$\Delta P_{ijrt\omega} \leq \Delta P_{ij(r-1)t\omega} \tag{44}$$

$$\Delta S_{ijrt\omega} - \Delta P_{ij(r-1)t\omega} \leq \mu_{ij(r-1)t\omega} \Delta S_{ijrt\omega} \tag{45}$$

$$\Delta P_{ijrt\omega} \leq (1 - \mu_{ij(r-1)t\omega}) \Delta S_{ijrt\omega} \tag{46}$$

$$\Delta Q_{ijrt\omega} \leq \Delta Q_{ij(r-1)t\omega} \tag{47}$$

$$\Delta S_{ijrt\omega} - \Delta Q_{ij(r-1)t\omega} \leq \eta_{ij(r-1)t\omega} \Delta S_{ijrt\omega} \tag{48}$$

$$\Delta Q_{ijrt\omega} \leq (1 - \eta_{ij(r-1)t\omega}) \Delta S_{ijrt\omega} \tag{49}$$

where $\mu_{ijrt\omega}$ and $\eta_{ij(r-1)t\omega}$ are the binary variables that indicate if the block is filled (0) or not (1).

References

[1] M. Korpaas, A.T. Holen, R. Hildrum, Operation and sizing of energy storage for wind power plants in a market system, Int. J. Electr. Power Energy Syst. 25 (8) (2003) 599–606.
[2] D.A. Halamay, T.K.A. Brekken, A. Simmons, S. McArthur, Reserve requirement impacts of large-scale integration of wind, solar, and ocean wave power generation, IEEE Trans. Sustainable Energy 2 (3) (2011) 321–328.
[3] M.A.O. Vázquez, D.S. Kirschen, Estimating the spinning reserve requirements in systems with significant wind power generation penetration, IEEE Trans. Power Syst. 24 (1) (2009) 114–124.
[4] A.K. Srivastava, A.A. Kumar, N.N. Schulz, Impact of distributed generations with energy storage devices on the electric grid, IEEE Syst. J. 6 (1) (2012) 110–117.
[5] H. Holttinen, et al., Design and operation of power systems with large amounts of wind power, in: Technical report, 2009, IEA Wind Task 25.
[6] V. Akhmatov, P.B. Eriksen, A large wind power system in almost island operation, a Danish case study, IEEE Trans. Power Syst. 22 (3) (2007) 937–943.
[7] R.H. Lasseter, Microgrids, in: Technical report, 2002.
[8] R.H. Lasseter, A. Abbas, M. Chris, J. Stephens, J. Dagle, R. Guttromson, A. Meliopoulous, R. Yinger, J. Eto, Integration of distributed energy resources. The CERTS microgrid concept, Lawrence Berkeley National Laboratory, 2002.
[9] J.A.P. Lopes, C.L. Moreira, A.G. Madureira, Defining control strategies for microgrids islanded operation, IEEE Trans. Power Syst. 21 (2) (2006) 916–924.
[10] L. Ding, F.M.G. Longatt, P. Wall, V. Terzija, Two-step spectral clustering controlled islanding algorithm, IEEE Trans. Power Syst. 28 (1) (2013) 75–84.
[11] G. Xu, V. Vittal, A. Meklin, J.E. Thalman, Controlled islanding demonstrations on the WECC system, IEEE Trans. Power Syst. 26 (1) (2011) 334–343.
[12] S.P. Chowdhury, S. Chowdhury, P.A. Crossley, UK scenario of islanded operation of active distribution networks with renewable distributed generators, Int. J. Electr. Power Energy Syst. 33 (7) (2011) 1251–1255.

[13] E. Álvarez, M.C. Antonio, P. Arboleya, A.J. Gutiérrez, Microgrid management with a quick response optimization algorithm for active power dispatch, Int. J. Electr. Power Energy Syst. 43 (1) (2012) 465–473.
[14] M.R. Aghamohammadi, A. Shahmohammadi, Intentional islanding using a new algorithm based on ant search mechanism, Int. J. Electr. Power Energy Syst. 35 (1) (2012) 138–147.
[15] M. Hasmaini, M. Hazlie, A. Ab Halim, W.P. Hew, A review on islanding operation and control for distribution network connected with small hydro power plant, Renewable Sustainable Energy Rev. 15 (8) (2011) 3952–3962.
[16] K.S. Meera, J. Sreedevi, K. Bavisetti, Umamaheswarrao, Design and real time performance evaluation of islanding and load shedding scheme, in: 2013 International Conference on Circuits, Controls and Communications, CCUBE, December 2013, pp. 1–6.
[17] A. El-Zonkoly, M. Saad, R. Khalil, New algorithm based on CLPS for controlled islanding of distribution systems, Int. J. Electr. Power Energy Syst. 45 (1) (2013) 391–403.
[18] P.A. Trodden, W.A. Bukhsh, A. Grothey, K.I.M. McKinnon, MILP formulation for controlled islanding of power networks, Int. J. Electr. Power Energy Syst. 45 (1) (2013) 501–508.
[19] P.A. Trodden, W.A. Bukhsh, A. Grothey, K.I.M. McKinnon, Optimization-based islanding of power networks using piecewise linear AC power flow, IEEE Trans. Power Syst. 29 (3) (2014) 1212–1220.
[20] I. Grau, L.M. Cipcigan, N. Jenkins, P. Papadopoulos, Microgrid intentional islanding for network emergencies, in: Proceedings of the 44th International Universities Power Engineering Conference, UPEC, September 2009, pp. 1–5.
[21] L. Jikeng, W. Xudong, W. Peng, L. Shengwen, S. Guanghui, M. Xin, X. Xingwei, L. Shanshan, Two-stage method for optimal island partition of distribution system with distributed generations, IET Gener. Transm. Distrib. 6 (3) (2012) 218–225.
[22] J. Allahdadian, A. Berizzi, C. Bovo, V. Ilea, M. Gholami, Islanding feasibility considering reactive power in the subtransmission systems, in: Proceedings of the 48th International Universities Power Engineering Conference, UPEC, September 2013, pp. 1–6.
[23] J. Allahdadian, A. Berizzi, C. Bovo, V. Ilea, M. Gholami, M. Merlo, A. Miotti, F. Zanellini, Detection of islanding feasibility in subtransmission systems, Int. Rev. Electr. Eng. (IREE) 8 (3) (2014).
[24] Q. Gemine, D. Ernst, B. Cornélusse, Active network management for electrical distribution systems: problem formulation and benchmark, CoRR, abs/1405.2806, 2014.
[25] K. Christakou, D.C. Tomozei, J.Y. Boudec, M. Paolone, AC OPF in radial distribution networks–parts I, II. CoRR, abs/1503.06809, 2015.
[26] C. Coffin, P. Van Hentenryck, A linear-programming approximation of AC power flows, INFORMS J. Comput. 26 (4) (2014) 718–734.
[27] M.C.O. Borges, J.F. Franco, M.J. Rider, Optimal reconfiguration of electrical distribution systems using mathematical programming, J. Control Autom. Electr. Syst. 25 (1) (2014) 103–111.
[28] A. Tabares Pozos, M. Lavorato de Oliveira, J.F. Franco Baquero, M.J. Rider Flores, A mixed-binary linear formulation for the distribution system expansion planning problem, in: Transmission & Distribution Conference and Exposition–Latin America, PES T&D-LA, September 2014, pp. 1–6.
[29] L.H. Macedo, J.F. Franco, M.J. Rider, R. Romero, Optimal operation of distribution networks considering energy storage devices, IEEE Trans. Smart Grid (99) (2015) 1.
[30] J.F. Franco, M.J. Rider, M. Lavorato, R. Romero, A mixed-integer LP model for the reconfiguration of radial electric distribution systems considering distributed generation, Electr. Power Syst. Res. 97 (2013) 51–60.
[31] I.A. Sajjad, G. Chicco, R. Napoli, Probabilistic generation of time-coupled aggregate residential demand patterns, IET Gener. Transm. Distrib. 9 (9) (2015) 789–797.
[32] Meteorología y climatología de Navarra, 2014. [online]. http://meteo.navarra.es/estaciones/mapadeestaciones.cfm.
[33] F. Spertino, P. Leo, I.S. Ilie, G. Chicco, DFIG equivalent circuit and mismatch assessment between manufacturer and experimental power-wind speed curves, Renew. Energy 48 (2012) 333–343.
[34] D. Pozo, J. Contreras, E.E. Sauma, Unit commitment with ideal and generic energy storage units, IEEE Trans. Power Syst. 29 (6) (2014) 2974–2984.
[35] B. Moradzadeh, K. Tomsovic, Mixed integer programming-based reconfiguration of a distribution system with battery storage, in: Proceedings of the North American Power Symposium, NAPS, September 2012, pp. 1–6.
[36] B. Moradzadeh, Optimal distribution reconfiguration and demand management within practical operational constraints (Ph.D. thesis), University of Tennessee, Knoxville, 2013.
[37] H.D. Chiang, R. Jean-Jumeau, Optimal network reconfigurations in distribution systems II. Solution algorithms and numerical results, IEEE Trans. Power Deliv. 5 (3) (1990) 1568–1574.
[38] Electricity demand tracking in real-time, associated generation mix and CO_2 emissions, 2014. [online]. https://demanda.ree.es/demandaeng.html.
[39] Mathwork. The mathworks inc. matlab, [available online]. http://www.mathworks.com/.
[40] A. Brooke, D. Kendrick, A. Meeraus, R. Raman, GAMS/CPLEX User Notes. GAMS Development Corp., Washington, D, 9.0. edition, 2003.
[41] M.R. Almassalkhi, I.A. Hiskens, Model-predictive cascade mitigation in electric power systems with storage and renewables-part I: Theory and implementation, IEEE Trans. Power Syst. 30 (1) (2015) 67–77.
[42] A.L. Motto, F.D. Galiana, A.J. Conejo, J.M. Arroyo, Network-constrained multiperiod auction for a pool-based electricity market, IEEE Trans. Power Syst. 17 (3) (2002) 646–653.
[43] M.R. Almassalkhi, Optimal distribution reconfiguration and demand management within practical operational constraints (Ph.D. thesis), University of Michigan, 2013.
[44] H. Zhang, V. Vittal, G.T. Heydt, J. Quintero, A relaxed AC optimal power flow model based on a taylor series, in: IEEE Innovative Smart Grid Technologies—Asia, ISGT Asia, 2013, pp. 1–5.